© Copyright, Princeton University Press. No part of this book may be distributed, posted, or reproduced in any form by digital or mechanical means without prior written permission of the publisher.

Contents

Preface **xi**

1 Introduction: The Role of Binary Star Evolution in Astrophysics **1**

2 Historical Notes on Binary Star Discoveries **10**
- 2.1 Visual Binaries and the Universal Validity of the Laws of Physics 10
- 2.2 Astrometric Binaries 11
- 2.3 Spectroscopic Binaries 14
- 2.4 Eclipsing Binaries 15
- 2.5 The Discovery of the Binary Nature of Novae and Other Cataclysmic Variables 17
- 2.6 The Discovery of the Binary Nature of the Brightest X-ray Sources in the Sky 20
- 2.7 Centaurus X-3: Discovery of the First Neutron Star X-ray Binary 21
- 2.8 Cygnus X-1: Discovery of the First Black Hole X-ray Binary 22
- 2.9 The Discovery of the Existence of Double NSs and Double BHs 25
- 2.10 The Discovery of Millisecond Radio Pulsars: Remnants of LMXBs 26
- 2.11 Type Ia, Ib, and Ic SNe: Results of the Evolution of Binary Systems 27
- 2.12 Binary Nature of Blue Stragglers, Barium Stars, and Peculiar Post-AGB Stars 29
- Exercises 31

3 Orbits and Masses of Spectroscopic Binaries **33**
- 3.1 Some Basics about Binary Orbits 33
- 3.2 Orbit Determination 36
- 3.3 Determination of Stellar Masses 41
- 3.4 Masses of Unevolved Main-sequence Stars 42
- 3.5 The Most Massive Stars 44
- 3.6 Falsification of Radial Velocity Curves 46
- 3.7 The Incidence of Interacting Binaries and Their Orbital Distributions and Masses 51
- Exercises 57

4 Mass Transfer and Mass Loss in Binary Systems **59**
- 4.1 Roche Equipotentials 59
- 4.2 Limitations in the Concept of Roche Equipotentials 63

© Copyright, Princeton University Press. No part of this book may be distributed, posted, or reproduced in any form by digital or mechanical means without prior written permission of the publisher.

4.3 Orbital Changes due to Mass Transfer and Mass Loss in Binary Systems 65
4.4 Observational Examples 83
4.5 Basic Physics of Mass Transfer via L_1 88
4.6 Accretion Disks 98
4.7 Tidal Evolution in Binary Systems 109
4.8 Common Envelopes 115
4.9 Eddington Accretion Limit 131
Exercises 134

5 Observed Binaries with Non-degenerate or White Dwarf Components 139
5.1 Introduction 139
5.2 Unevolved Systems 142
5.3 Evolved Systems with Non-degenerative Components 143
5.4 Systems with One or Two White Dwarfs 152
Exercises 167

6 Observed Binaries with Accreting Neutron Stars and Black Holes: X-ray Binaries 168
6.1 Discovery of NS and BH Character of Bright Galactic X-ray Sources 168
6.2 Two Types of Persistent Strong X-ray Sources: HMXBs and LMXBs 176
6.3 HMXBs and LMXBs vs. IMXBs 180
6.4 Determinations of NS Masses in X-ray Binaries 188
6.5 BH X-ray Binaries 191
6.6 Binaries and Triples with Non-interacting BHs 206
Exercises 209

7 Observed Properties of X-ray Binaries in More Detail 213
7.1 High-mass X-ray Binaries in More Detail 213
7.2 Stellar Wind Accretion in More Detail 227
7.3 Spin Evolution of Neutron Stars 232
7.4 The Corbet Diagram for Pulsating HMXBs 243
7.5 Orbital Changes due to Torques by Stellar Wind Accretion, Mass Loss, and Tides 245
7.6 Measuring BH Spins in X-ray Binaries 245
7.7 Ultra-luminous X-ray Binaries 252
7.8 Low-mass X-ray Binaries in More Detail 258
Exercises 270

8 Evolution of Single Stars 271
8.1 Overview of the Evolution of Single Stars 271
8.2 Final Evolution and Core Collapse of Stars More Massive than 8 $M_\odot$ 299

© Copyright, Princeton University Press. No part of this book may be distributed, posted, or reproduced in any form by digital or mechanical means without prior written permission of the publisher.

8.3 Evolution of Helium Stars 315
Exercises 325

9 Stellar Evolution in Binaries 326
9.1 Historical Introduction: Importance of Mass Transfer 326
9.2 Evolution of the Stellar Radius and Cases of Mass Transfer 327
9.3 RLO: Reasons for Large-scale Mass Transfer and Conditions for Stability of the Transfer 334
9.4 Results of Calculations of Binary Evolution with Conservative Mass Transfer 340
9.5 Examples of Non-conservative Mass Transfer 353
9.6 Comparison of Case B Results with Some Observed Types of Systems 360
9.7 Differences in Final Remnants of Mass-transfer Binaries and Single Stars 366
9.8 Slowly Rotating Magnetic Main-sequence Stars: The Products of Mergers? 371
Exercises 374

10 Formation and Evolution of High-mass X-ray Binaries 376
10.1 Introduction: HMXBs are Normal Products of Massive Binary Star Evolution 376
10.2 Formation of Supergiant HMXBs 376
10.3 Formation of B-emission (Be)/X-ray Binaries 379
10.4 WR Binaries, HMXBs, and Runaway Stars 386
10.5 Stability of Mass Transfer in HMXBs 393
10.6 The X-ray Lifetime and Formation Rate of the Blue Supergiant HMXBs 395
10.7 Highly Non-conservative Evolution and Formation of Very Close Relativistic Binaries 403
10.8 Formation Models of HMXBs Different from Conservative Case B Evolution 408
10.9 The Lower Mass Limit of Binary Stars for Terminating as a BH 411
10.10 Final Evolution of BH-HMXBs: Two Formation Channels for Double BHs 414
10.11 Final Evolution of Wide-orbit BH-HMXBs via CE Evolution 415
10.12 Final Evolution of Relatively Close-orbit BH-HMXBs via Stable RLO 419
10.13 Refinement of the DNS Formation Model: Case BB RLO in Post-HMXB Systems 423
Exercises 431

11 Formation and Evolution of Low-mass X-ray Binaries 433
11.1 Origin of LMXBs with Neutron Stars 433
11.2 Origin of LMXBs with Black Holes 449

© Copyright, Princeton University Press. No part of this book may be distributed, posted, or reproduced in any form by digital or mechanical means without prior written permission of the publisher.

11.3 Mechanisms Driving Mass Transfer in Close-orbit LMXBs and CVs 450
11.4 Formation and Evolution of UCXBs 464
11.5 Mechanisms Driving Mass Transfer in Wide-orbit LMXBs and Symbiotic Binaries 470
11.6 Stability of Mass Transfer in Intermediate-Mass and High-Mass X-ray Binaries 475
Exercises 477

12 Dynamical Formation of Compact Star Binaries in Dense Star Clusters 480
12.1 Introduction 480
12.2 Observed Compact Object Binaries in Globular Clusters: X-ray Binaries and Radio Pulsars 482
12.3 Possible Formation Processes of NS Binaries in Globular Clusters 483
12.4 Dynamical Formation of Double BHs 489
12.5 Compact Objects in Globular Clusters Constrain Birth Kicks 492

13 Supernovae in Binaries 495
13.1 Introduction 495
13.2 Supernovae of Type Ia 498
13.3 Stripped-Envelope Core-Collapse SNe 513
13.4 Electron-capture SNe in Single and Binary Stars 518
13.5 Ultra-Stripped Supernovae 523
13.6 Comparison between Theory and Observations of SNe Ib and Ic 529
13.7 Supernova Kicks 531
13.8 Kinematic Impacts on Post-SN Binaries 541
Exercises 556

14 Binary and Millisecond Pulsars 560
14.1 Introduction to Radio Pulsars 561
14.2 To Be Recycled or Not to Be Recycled 571
14.3 MSPs with He WD or Sub-stellar Dwarf Companions–Evolution from LMXBs 578
14.4 MSPs with CO WD Companions–Evolution from IMXBs 591
14.5 Formation of MSPs via Accretion-induced Collapse 595
14.6 Recycling of Pulsars 597
14.7 Masses of Binary Neutron Stars 618
14.8 Pulsar Kicks 635
14.9 Formation of Double Neutron Star Systems 637
Exercises 648

15 Gravitational Waves from Binary Compact Objects 652
15.1 The Evidence of GWs prior to LIGO 655
15.2 GW Luminosity and Merger Timescale 658

© Copyright, Princeton University Press. No part of this book may be distributed, posted, or reproduced in any form by digital or mechanical means without prior written permission of the publisher.

15.3 Observations of GW Signals from Binaries 661
15.4 Galactic Merger Rates of Neutron Star/Black Hole Binaries 664
15.5 Formation of Double Black Hole Binaries 667
15.6 Properties of GW Sources Detected so Far 678
15.7 Empirical Merger Rates 694
15.8 BH Spins–Expectations and Observations 696
15.9 Anticipated Other Sources to be Detected in the GW Era 706
15.10 GW Follow-up Multimessenger Astronomy 712
15.11 Cosmological Implications 718
15.12 LISA Sources 718
15.13 LISA Sensitivity Curve and Source Strain 730
Exercises 736

16 Binary Population Synthesis and Statistics 739
16.1 Introduction 739
16.2 Methodology of Population Synthesis 741
16.3 Empirical vs. Binary Population Synthesis-Based Estimates of Double Compact Object Merger Rates 747
16.4 Some History of Early Binary Population Synthesis: Evolution of Open Star Clusters with Binaries 753

Acknowledgments 761

Answers to Exercises 765

List of Acronyms 767

References 771

Index 843

© Copyright, Princeton University Press. No part of this book may be distributed, posted, or reproduced in any form by digital or mechanical means without prior written permission of the publisher.

Chapter One

Introduction

The Role of Binary Star Evolution in Astrophysics

Many key astrophysical objects and phenomena are related to the evolution of binary stars. This holds, for example, for the formation of the brightest X-ray sources in the sky and the formation of double neutron stars (NSs) and black holes (BHs), the mergers of which produce the strongest bursts of energy anywhere in the observable Universe, measurable on Earth with gravitational wave (GW) detectors.[1] Binary interactions also play a role for the origin of most supernovae (SNe), all nova explosions and short gamma-ray bursts, and the formation of millisecond radio pulsars and a large variety of stars with peculiar chemical abundances, such as barium stars and carbon-enriched metal poor stars.

It has been long realized, from the fact that most stars are members of binary systems (Abt & Levy, 1976; Bonnell et al., 2003), that binary evolution must play a key role in stellar evolution (e.g., van den Heuvel, 1994a). This early and important awareness has even been strengthened further by the findings of, for example, Chini et al. (2011) and Sana et al. (2012) that practically all massive stars are found in binaries with orbits such that at some stage in their evolution, the far majority of these stars will interact with each other. This implies that binary interactions dominate the evolution of massive stars.

The first ideas about the evolution of binary systems originated in the 1950s. They were largely inspired by the surprising characteristics of Algol-type eclipsing binary systems (see also Section 2.4). Here, *Algol-type* means physically similar to the Algol system, which consists of an unevolved B8V[2] main-sequence star with a mass of $3.2\,M_\odot$ together with an evolved but less massive subgiant companion star of spectral type K3 IV of mass $0.7\,M_\odot$. This situation, with the more evolved star having the smaller mass of the two, is just opposite to what one would expect on the grounds of stellar evolution, as stars of larger mass are expected to have shorter lives than stars of smaller mass do. In a binary—where both stars were born at the same time—one would therefore expect the star of larger mass to be in a more advanced stage of evolution at any time than that of its companion of smaller mass.

---

[1] The first ever detected BH merger event GW150914 (Abbott et al., 2016d) released an energy of $3\,M_\odot\,c^2$ within a fraction of a second, thereby outshining all stars in the Universe for a brief moment.

[2] B8V refers to a star of spectroscopic type B8 and luminosity class V.

© Copyright, Princeton University Press. No part of this book may be distributed, posted, or reproduced in any form by digital or mechanical means without prior written permission of the publisher.

This is what is called the *Algol paradox*. Crawford (1955) was the first to realize that this paradoxical situation can be explained if one assumes that large-scale mass transfer can take place during the evolution of a binary system: Crawford hypothesized that the subgiant components in Algol-type binaries were originally the more massive components of these systems. As the more massive star evolved faster than its less massive companion did, it was the first one to exhaust the hydrogen fuel in its core and evolve into a giant star with a much expanded envelope. The presence of the close companion, however, prevented such an evolution: when the outer layers of the expanding (sub)giant came under the gravitational influence of the companion, they were captured by this smaller star (the *accretor*), causing the accretor to increase in mass at the expense of the (sub)giant (the *donor*). The (sub)giant transferred so much of its mass that it was finally able to restabilize its internal structure. At that moment, it became the less massive of the two stars, and the originally less massive star became the most massive one of the pair.

The first attempt to carry out a real calculation of this type of evolution with mass transfer was by Morton (1960). He demonstrated the correctness of Crawford's conjecture that mass transfer, once it begins, continues until the (sub)giant has become the less massive star of the system. In his calculations, however, Morton still assumed that the orbital period of the system does not change during the mass transfer. This is not correct because, if one assumes that the total mass of the system is conserved, one also expects the total angular momentum of the system to be conserved. The total angular momentum is, in good approximation, equal to the orbital angular momentum (as the rotational angular momentum of the two stars is usually much smaller than the orbital one). Conservation of the orbital angular momentum implies that during the mass transfer the orbital period and separation change in a well-determined way, which will be explained in Chapter 4. The evolution of close binaries in this more realistic approach was first calculated, independently of one another, by Paczyński (1966), Kippenhahn & Weigert (1967), and Plavec (1967). Their work was the foundation of all subsequent work on the evolution of close binary systems. Furthermore, the discovery of the first celestial X-ray source in 1962 and of the X-ray binaries in 1971–1972—which earned Riccardo Giacconi the 2002 Physics Nobel Prize—has given a great stimulus to the research in this field. The X-ray binaries consist of a normal star together with a compact object: a NS or a BH, which are the end states of evolution of massive stars. The X-rays from these binaries, which are observed with space-borne detectors, are generated by the accretion of matter onto the compact star, which is captured from the outer layers of the companion star. During the accretion this gas, falling inward in the extremely strong gravitational field of the compact star, is heated by the release of gravitational potential energy to temperatures above 10^6 K, causing it to emit X-rays.

Without the occurrence of extensive mass transfer from the original primary star (the progenitor of the compact object) to the secondary star, most of these systems could not have survived the SN explosion of the primary star in which the NS or BH was formed (van den Heuvel & Heise, 1972; Tutukov & Yungelson, 1973b), because the probability of the post-SN orbit to remain bound depends on the relative mass loss from the system during the SN (see e.g. Section 4.3.10 and Chapter 13).

© Copyright, Princeton University Press. No part of this book may be distributed, posted, or reproduced in any form by digital or mechanical means without prior written permission of the publisher.

Since the early 1970s, the realization of the importance of accretion of matter onto a compact star (NS, BH, or white dwarf [WD]) as an energy source in many types of binaries, ranging from X-ray binaries to cataclysmic variables (CVs) and symbiotic stars, has been a further important source of inspiration for new research on the structure and evolution of close binary systems. The discoveries since 1974 of binary radio pulsars, of which at least 20 are double NSs (DNSs; for a recent review, see Tauris et al., 2017), have revealed many interesting properties, including the many relativistic effects that are measurable in them with unprecedented precision (e.g., Taylor & Weisberg, 1989; Taylor, 1992; Kaspi & Kramer, 2016).

These discoveries have created a new and fundamental branch of relativistic binary star astrophysics, which among other things has produced the most accurate measurements of masses of any stellar objects so far (Chapter 14). The measured rate of orbital decay of the first-discovered double NS, PSR B1913+16, is in exact agreement with the decay rate predicted from the emission of GWs according to the general theory of relativity. The highly precise detection of this and other relativistic effects earned the discoverers of this binary pulsar, Russell Hulse and Joseph Taylor, the 1993 Physics Nobel Prize. Later-discovered DNSs, particularly the double pulsar system J0737−3039, have further refined the up to five tests of relativity allowed by these systems (Section 14.7.1) to almost incredible precision (Wex, 2014; Kramer et al., 2021).

The amazing discoveries of the merger event of a double BH, starting with GW-150914 in September 2015 (Abbott et al., 2016d), and of a DNS, in August 2017 (Abbott et al., 2017c), have revealed the ultimate final destiny of a massive binary star system and demonstrated the production of strong bursts of GWs, that are observable on Earth. This earned the LIGO pioneers Rainer Weiss, Kip Thorne, and Barry Barish the 2017 Physics Nobel Prize. But how do ordinary stars born in a binary system end up as two NSs or BHs that finish as a final single BH remnant? To answer this question, we need to follow the binary system through a long chain of exotic binary interactions (Fig. 1.1), involving mass transfer between the stellar components, SNe, and relativistic effects. That the orbits of evolved massive stars in binaries will shrink to the very small sizes observed for the double compact objects was predicted before these objects were discovered (van den Heuvel & De Loore, 1973).

Radio pulsars are some of the most intriguing astrophysical objects, among which a sizable fraction of binaries is found with quite special characteristics that give important information on binary evolution. To understand the continuously growing diversity of observed radio pulsars (see Fig. 1.2), it is necessary to link their properties to the stellar and binary evolution of their progenitors (Bhattacharya & van den Heuvel, 1991).

The detection of close binary pulsars and of the merger events of double BHs and NSs have further increased the interest in the evolution of binary systems. These discoveries demonstrated that, even though binaries may have undergone several stages of mass transfer during their evolution, where up to 90% of their original mass and >95% of their original orbital angular momentum is lost from the system, and despite having experienced two SN explosions, the two stars might still survive as a (very close) binary system with two compact objects.

© Copyright, Princeton University Press. No part of this book may be distributed, posted, or reproduced in any form by digital or mechanical means without prior written permission of the publisher.

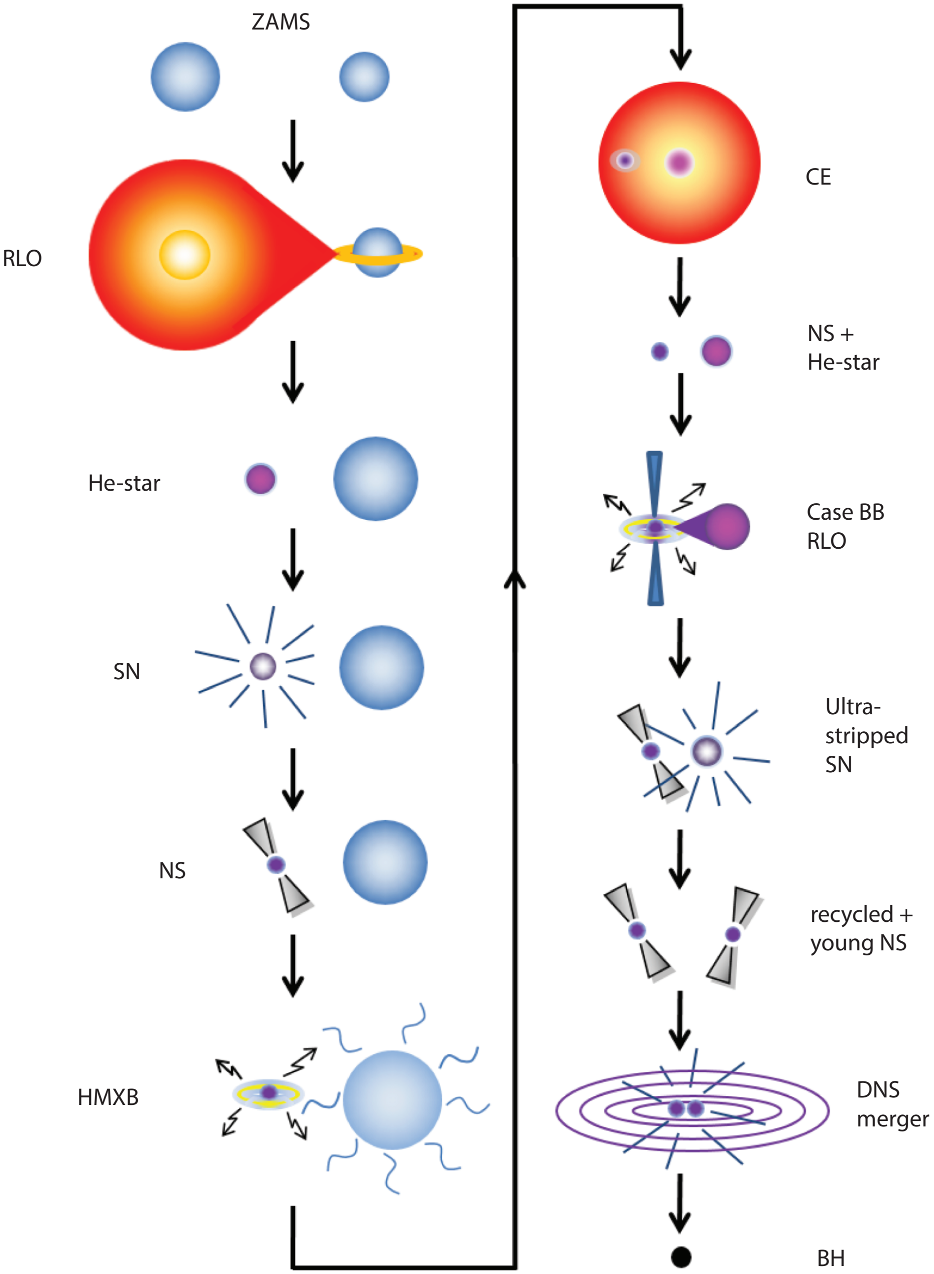

Figure 1.1. Formation model of a close double neutron star (DNS) system as final product of the evolution of a massive close binary. The DNS system may eventually merge and leave a solitary BH remnant. The same model, scaled up to higher initial stellar masses, is one of the main scenarios to explain the formation of double BHs (see Chapters 10, 12, and 15). After Tauris et al. (2017).

For general queries, contact webmaster@press.princeton.edu

© Copyright, Princeton University Press. No part of this book may be distributed, posted, or reproduced in any form by digital or mechanical means without prior written permission of the publisher.

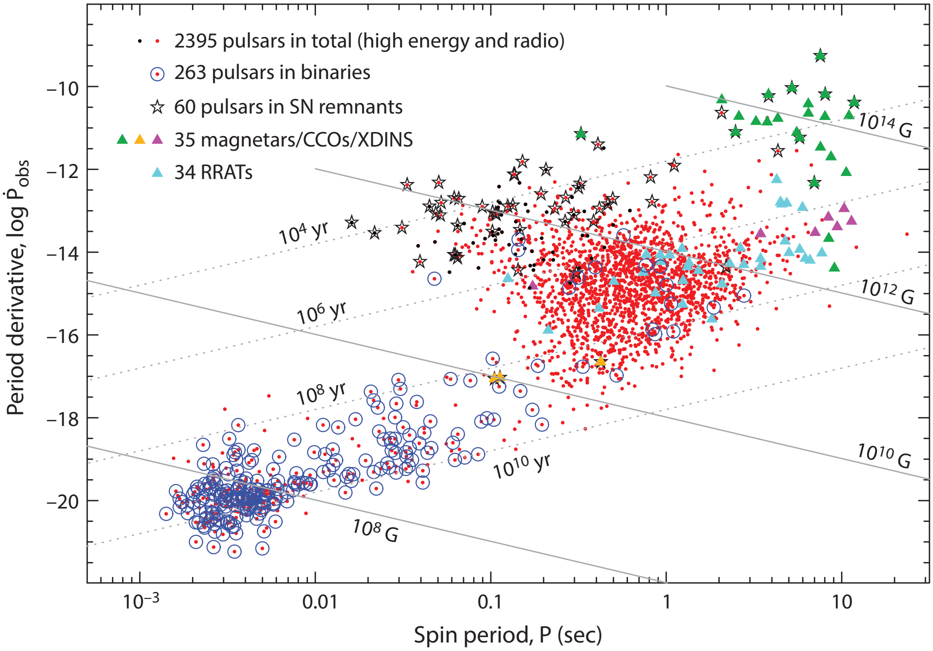

Figure 1.2. Observed population of ∼2,400 radio and high-energy pulsars with measured values of both spin period (P) and period derivative ($\dot{P}$). The variety of pulsars has flourished immensely since their discovery in 1967 and continues to be a major science driver in modern astrophysics. Binary pulsars (blue circles) dominate among the fast-spinning millisecond pulsars. CCOs are central compact objects of SN remnants, XDINs are X-ray dim isolated NSs, and RRATs are rotating radio transients (see Chapter 14). Data taken from the *ATNF Pulsar Catalogue* in June 2021 (Manchester et al., 2005, https://www.atnf.csiro.au/research/pulsar/psrcat).

The existence of the close double NSs and close double BHs has also demonstrated that a precise knowledge of the physics of binary evolution is of vital importance for understanding fundamental astrophysics as diverse as the generation of the strongest bursts of GW radiation, the production of gamma-ray bursts, and the synthesis of heavy r-process (or rapid neutron-capture) elements in the Universe. The latter was predicted to be produced by the merging of double NSs or NS+BH binaries (Lattimer & Schramm, 1976) and expected to be observable as a so-called kilonova optical-infrared eruption (Metzger et al., 2010; Berger, 2014).

These predictions have been beautifully confirmed by the spectroscopic study of the optical-infrared transient that accompanied the DNS merger event GW170817 (Abbott et al., 2017c, 2017d, 2017e). The mergers of double compact object binaries with at least one NS also had been predicted to produce gamma-ray bursts (Paczynski, 1986; Eichler et al., 1989), which was confirmed by the Fermi and INTEGRAL missions by the detection of a short gamma-ray burst, following within 2 sec after GW170817

© Copyright, Princeton University Press. No part of this book may be distributed, posted, or reproduced in any form by digital or mechanical means without prior written permission of the publisher.

(Abbott et al., 2017a; Savchenko et al., 2017). The occurrence of an electromagnetic counterpart—the kilonova—is a great advantage of a DNS merger or a NS+BH merger, relative to the mergers of double BHs, because this allows one to determine the place of origin of the merger on the sky with sub-arcsecond precision. In the case of GW170817, this place turned out to be in the lenticular (S0) Galaxy. NGC 4993 at a distance of 40 Mpc (Coulter et al., 2017; Soares-Santos et al., 2017). The discovery, in this way, of the DNS merger GW170817 at once provided the solution to the nature of a variety of key astrophysical phenomena.

In the past decades it was realized that the SNe of Types Ia, Ib, and Ic (characterized by the absence of hydrogen in their spectra) most likely are related to the evolution of binary systems (see Section 2.10). That these three types together form approximately half of all SNe shows how important knowledge of binary star evolution is for a general understanding of observational stellar evolution processes.

Finally, in the past decades it was discovered that binary evolution has affected a large variety of low- and intermediate-mass stars with peculiar abundances of chemical elements. Examples are the barium stars, which are G and K giants with masses up to a few solar masses and an overabundance of barium and other s-process elements (products of slow neutron-capture processes) (Bidelman & Keenan, 1951; Boffin & Jorissen, 1988). They are wide binaries with eccentric orbits and orbital periods ranging from approximately 100 to 10,000 days (Boffin & Jorissen, 1988). The binary nature of these stars, of blue stragglers in star clusters, of extremely metal-depleted post–asymptotic giant branch stars, of carbon-enhanced metal-poor (CEMP) stars, and of $>80\%$ of nuclei of planetary nebulae was discovered in past decades. These discoveries show that the evolution of $\sim 50\%$ of all low- and intermediate-mass stars is expected to be affected by binary evolution (Abate et al., 2015). Because lower-mass stars are far more abundant in galaxies than massive stars are, the products of low- and intermediate-mass binaries are expected to vastly outnumber the products of the evolution of massive binaries. However, in this book we will concentrate mainly on the physics and evolution of the more massive binaries that produce NSs and BHs and on the origin of Type Ia SNe, which are caused by exploding WDs and are of crucial importance for cosmology.

In the last decades it was realized that stars are found often, even in triple systems or higher-order multiple systems. Observational estimates suggest that approximately 20%–30% of all binary stars are members of triple systems (Tokovinin et al., 2006; Rappaport et al., 2013). These systems may remain bound with a long-term stability in a hierarchical structure (a close inner binary with a third star in relatively distant orbit). Since the 1970s, a number of stability criteria for a triple system have been proposed (see Mikkola, 2008, for an overview) that enable predictions for the long-term stability of triple systems. Iben & Tutukov (1999) estimated that in $\sim 70\%$ of the triple systems, the inner binary is close enough that the most massive star will evolve to fill its Roche lobe. Furthermore, in $\sim 15\%$ of the triple star systems, the outer third (tertiary) star may even also fill its Roche lobe at some point, possibly leading to disintegration or production of rare configurations with three degenerate objects in the same system. In 2014, Ransom et al. (2014) reported the remarkable discovery of a triple-system pulsar (PSR J0337+1715), which is exactly the first example of such

© Copyright, Princeton University Press. No part of this book may be distributed, posted, or reproduced in any form by digital or mechanical means without prior written permission of the publisher.

an exotic system—a NS orbited by two WDs. (For a formation and evolution scenario for this complex system, which must have survived a SN explosion and at least three stages of mass transfer between the stellar components, see our model in Tauris & van den Heuvel [2014].) Besides specific triple-star interactions, such as Kozai-Lidov resonances (Kozai, 1962; Lidov, 1962) and the above-mentioned dynamical stability considerations, most interactions between stars in triples are similar to the interactions between binary stars. For this reason, we focus only on binary stars in this book.[3]

The 2020s and 2030s are expected to reveal a large number of discoveries of new double compact object systems, as well as their progenitors and merger remnants. This field of astrophysics is strongly driven by investments in new big-science instruments. The Square-Kilometer Array (SKA) is expected to increase the number of known radio pulsars by a factor of 5 to 10, thus resulting in a total of >100 known DNS systems (Keane et al., 2015). The Five-hundred-meter Aperture Spherical Telescope is also expected to contribute a significant number of new radio pulsars (Smits et al., 2009; Nan et al., 2011), including new discoveries of pulsar binaries. High-mass X-ray binaries (HMXBs), the anticipated progenitors of double compact object systems containing NSs and BHs, are continuously being discovered with ongoing X-ray missions (INTEGRAL, Swift, XMM-Newton, and Chandra [see e.g., Chaty, 2013]). New and upcoming space-borne X-ray telescopes such as eXTP, STROBE-X, and Athena are expected to produce further discoveries of these systems. Hence, we are currently in an epoch when a large wealth of new information on exotic binaries is becoming available. In light of this, it is important to explore and understand the formation and evolution of such binary systems in more detail. Earlier textbooks on binary evolution are those of Shore et al. (1994), Hilditch (2001), and Eggleton (2006), to which we refer for further reading. For an earlier book on physics and evolution of relativistic objects in binaries, we refer to Colpi et al. (2009).

This book is organized as follows. In Chapter 2, we give a brief history of the discovery of the different types of binary systems and, where appropriate, summarize their importance in modern astrophysics. In Chapter 3, we consider how the orbital parameters of spectroscopic and eclipsing binaries are measured and, how from these measurements information is obtained about the masses and radii of the stars. We give an overview of the thus-derived masses of stars of different spectral types.

In Chapter 4, we consider basic aspects of the celestial mechanics of binary systems, the meaning and limitations of the Roche-lobe concept, as well as the changes in orbital period and binary separation that are induced by various processes of mass loss and mass transfer in binary systems. We first consider the somewhat idealized "conservative" evolution, in which the total mass and orbital angular momentum of the binary are expected to be conserved during the evolution, followed by the more realistic and exotic types of close binary evolution, so-called non-conservative evolution, in which large losses of mass and orbital angular momentum from the systems are taken into account. A treatment of common envelopes and the orbital evolution during the

---

[3] Formation of stellar binaries via triple- or quadruple-star dynamical interactions in dense cluster, however, are discussed in Chapter 12. For a recent review on the evolution of destabilized triple systems, see Toonen et al. (2022).

© Copyright, Princeton University Press. No part of this book may be distributed, posted, or reproduced in any form by digital or mechanical means without prior written permission of the publisher.

dynamically unstable in-spiral phase are described as well. Finally, we briefly discuss the Eddington accretion limit as well as accretion disks.

In Chapter 5, we describe the observed properties and the general classifications of the various types of interacting binary systems that do not contain NSs or BHs, concentrating mostly on systems in which at least one component is an evolved star, that is, a (sub)giant, or a WD.

In Chapters 6 and 7, we describe the observed properties of X-ray binaries: HMXBs as well as low-mass X-ray binaries (LMXBs), including mass determination of the accreting NSs and BHs. Regarding HMXBs, we discuss Be-star X-ray binaries, supergiant X-ray binaries, and, for example, stellar wind accretion and the Corbet diagram. We also discuss the recently discovered class of pulsating ultra-luminous X-ray sources. For LMXBs, we discuss the various types, including the systems with BHs and the symbiotic X-ray binaries with accreting NSs.

In Chapter 8, we give an overview of the evolution of single stars (with a special focus on the final evolution of massive stars). In Chapter 9, we apply this knowledge to the evolution of binaries in general. Here, we also discuss in detail the various cases of mass transfer (including mass loss) and orbital stability analysis, and we end with a comparison between the outcomes of single vs. binary star evolution.

This knowledge is crucial for understanding the formation and evolution of X-ray binaries, which are the subjects of Chapters 10 (HMXBs) and 11 (LMXBs). We discuss the final stages of HMXBs (including Wolf-Rayet [WR] star binaries), with or without a common envelope, leading to the formation of double NS/BH binaries. For LMXBs and CVs, we also discuss the mechanisms driving the mass transfer in LMXBs and CVs. These concern the internal evolution of the companion star, as well as the loss of orbital angular momentum due to emission of GWs and/or a magnetically coupled stellar wind, or a combination of these. We also discuss the final mass-transfer stage from WDs in very tight binaries, in the so-called AM Canum Venaticorum (double WD) systems and the ultra-compact X-ray binary sources (typically WD+NS systems).

Binaries with compact objects can also be formed by the dynamical evolution of dense star clusters. This is the subject of Chapter 12.

Chapter 13 concerns SNe in binaries. We first discuss the evolution leading to the thermonuclear Type Ia SNe, triggered by the accretion of matter by a WD, and we also consider accretion-induced collapse (AIC) of massive WDs. We subsequently discuss the origin of Type Ib/Ic SNe and the evidence derived from theoretical computations of the late stages of close binary evolution, including ultra-stripped SNe, combined with observations of SN light curves and known Galactic post-SN DNS systems. We discuss the evidence for momentum kicks imparted onto compact objects during various SN events (iron core collapse and electron-capture SNe) and examine the kinematical effects of these kicks on the resulting compact-object binaries.

In Chapter 14, using the results of the previous chapters, the final stages of the formation of binary and millisecond radio pulsars is studied; in other words, the transition from X-ray binaries to radio pulsars. We review the recycling of pulsars in detail, including the accretion torques at work. We review the rich diversity of resulting millisecond pulsar binaries and their component masses (theoretical expectations and

For general queries, contact webmaster@press.princeton.edu

© Copyright, Princeton University Press. No part of this book may be distributed, posted, or reproduced in any form by digital or mechanical means without prior written permission of the publisher.

measurements via relativistic effects). Finally, we revisit the formation of double NS (DNS) systems.

Chapter 15 is devoted to GW astrophysics. We cover the basic physics of GW emission and detection. We discuss formation channels of both high-frequency (LIGO–Virgo–KAGRA–IndIGO) and low-frequency (LISA and TianQin) GW sources. We review the signals expected from extragalactic merging double BHs and NSs, including the electromagnetic counterparts of these mergers, and the Galactic WD and NS binaries as continuous GW emission sources. The different models for the formation of the double BHs are discussed in depth in light of the latest observations of "ordinary" and exotic events from the LIGO–Virgo-KAGRA network.

Chapter 16 discusses the subject of binary population synthesis with an emphasis on methodology and statistics. Two examples are highlighted that illustrate a synthetic open star cluster population of binaries and the differences between estimates of empirical vs. theoretical double NS (DNS) merger rates.

© Copyright, Princeton University Press. No part of this book may be distributed, posted, or reproduced in any form by digital or mechanical means without prior written permission of the publisher.

Index

absolute magnitude, 31
absolute orbit, 12, 34
accreting X-ray millisecond pulsars, 24, 26, 263–266, 560
accretion, 2, 3, 27; Eddington limit, 75, 131–133; energetics of, 170; as energy source in X-ray binaries, 170; four stages, 232ff; hypercritical (*see* common envelope, hypercritical accretion on NS); propeller phase, 234–236; quasi-spherical, 236ff; settling, 231–233; spherical onto black hole, 107–109; torque, 236ff, 598
accretion, stellar wind, 72, 184–188, 227–231; Bondi-Hoyle-Lyttleton, 228–231; disk formation, 241; instabilities, 241
accretion disk, 20, 23, 597ff; formation, 98–103; formation in wind, 241; heating, 104ff; instabilities, 20, 105–106; location, 99; maximum size, 103ff
accretion-induced collapse, 8, 436–447, 595–597
AGB stars, 163, 164, 328
Alfvén radius/surface, 233ff
Algol paradox, 2, 16, 326
Algol-type binaries, 1,16, 142, 144, 146, 326
aLIGO 708. *See also* LIGO
AM Canum Venaticorum stars, 158–160, 460–462
Anomaly: eccentric, 39; mean, 39; true, 39
Ap, Bp stars, possible origins, 371–374
apastron, 37ff
apparent magnitude, 31
Applegate mechanism, 81ff
apsidal motion, 112
Ariel 5, 21
association (of OB stars), 389–395
astrometric binaries, 11, 13
Athena, 7

Baade, W., 495
Barish, B., 3, 625
barium stars, 6, 29, 30, 163, 164
barycenter, 34, 35
Bessel, F. W., 11
Be-stars, 213–216, 759
B[e] supergiants, 219–221, 295–297
Beta Lyrae, 17, 84, 141, 142, 361
Be/X-ray binaries. *See* high-mass X-ray binaries (HMXBs)
binary distribution: of mass ratios, 55ff, 741–743; of orbital periods, 53ff, 741–743; of primary masses, 54ff, 741–743
binary evolution: Cases of mass transfer, 328–330, 332, 333; Case A, examples of outcome, 341–342, 409–410; Case B, examples of outcome, 342–351; Case B comparison outcomes, with observations, 360ff; Case C, 358–359, 412–414; Case AB, example, 357–358; Case BB, examples, 351–353; Case BB, to a NS companion, 425–431; conservative (mass transfer), 8, 72, 334–335; difference of outcome, compared to single-star evolution, 366–371; non-conservative evolution, examples, 353–358; response of secondary, 351
binary evolution, reasons for large-scale mass transfer of, 334ff; for donor with convective envelope, 336; for donor with radiative envelope, 335–336
binary evolution, stability of mass transfer of: criteria for stable mass transfer of, 336, 339; donor with convective

© Copyright, Princeton University Press. No part of this book may be distributed, posted, or reproduced in any form by digital or mechanical means without prior written permission of the publisher.

binary evolution (*continued*) envelope, 336; donor with radiative envelope, 335, 336

binary fraction of stars, 51ff, 741–743

binary incidence of interacting, 51ff, 741–743

binary population synthesis, 739ff: double-compact star merger rates of, 747–752; history of, 753–754; methodology of, 741–747; pitfalls of, 747

binary radio pulsar(s). *See* pulsars (radio)

black holes (BHs): kicks (*see* supernovae, kicks from); masses, 194–197, 652ff; mergers (*see* mergers: black holes); microquasar, 197ff; non-interacting, 206–209; number in the Galaxy, 206; spherical accretion, 107–109; spin, 245–252, 696–707; threshold mass for BH production by stellar evolution, 305ff, 411–412; X-ray novae, 193–196. *See also* double black holes

black holes, formation of: in binaries, 406, 411–414, 449–450; in single stars, 305ff

black holes, in X-ray binaries (low- and high-mass), 195–197: formation of, 406, 411–414, 449–450. *See also* high-mass X-ray binaries

black-widow systems, 87, 562. *See also* pulsars (radio)

blueshift, 14

blue stragglers, 6, 29, 30, 753–759

blue supergiants: evolutionary state of, 399–400; mass loss, 284–289

Bondi-Hoyle-Lyttleton accretion, 228–231

Brahe, Tycho, 33

Bright Star Catalogue, 15

brown dwarfs, 87. *See also* ultra-compact X-ray binaries

Bunsen, R., 11

burst oscillations, 265–266

Carbon-enhanced metal-poor (CEMP) stars, 6, 163

Cases A, B, C, etc. of close binary evolution, 329, 332–333. *See also* binary evolution

Castelli, Benedetto, 10

Castor AB, 11, 15

cataclysmic variables, 3, 153–154: model calculations of evolution, 460–462; orbital period distribution, 153, 458; orbital period gap, 457; orbital period minimum, 458–460; pre-orbital period minimum, 154–155

CCOs, 5, 562

CE. *See* common envelope

CEMP stars, 164

Centauris X-3, 21–22, 171, 176

Cepheids, 17

Chandra, 7

Chandrasekhar limit, 29

Chemically homogeneous evolution, 673–676

chemically polluted stars, 29, 164

CH-stars, 164

circumbinary disk, 76ff

Clark, A. G., 12

cluster (of stars): globular (*see* globular clusters); open, with binary evolution, 753–759

common envelope (CE), 8, 116ff; additional energy sources, 126–128; binding energy, 122–125; coalescence of (merger), 122; ejection, 118ff, 122ff, 125ff; ejection formation, 115ff; HMXBs, 117ff, 122, 404–408; HMXBs, hypercritical accretion on NS, 128; jets, 127; limitations, for formation of double BHs, 414–419; main phases of, 117ff; observational evidence of, 128–130; post-CE evolution, 123, 124, 406, 415ff, 434–438, 446, 449–450, 637–641, 670–672, 722ff; post-CE separation, 116, 122ff, 124, 405–407; recombination energy of, 126; red novae, 128–130; spiral-in, 115, 117ff; wide massive binaries, 449–450

compactness parameter, of stellar core, 306

conservative evolution. See binary evolution

contact binaries, 139, 141

Conti scenario: for forming WR stars, 294–298; and red supergiants, 296–298

Corbet diagram: of HMXBs, 243–244; of radio-pulsar binaries, 577

© Copyright, Princeton University Press. No part of this book may be distributed, posted, or reproduced in any form by digital or mechanical means without prior written permission of the publisher.

core-collapse supernovae. *See* supernovae, core collapse of
co-rotation radius, 234ff
Cosmic Explorer, 708
Crab Nebula, 26, 561
Cygnus X-1, 21, 23, 174, 176, 179, 198, 199, 412–414
Cygnus X-1 Formation, 412–414
Cygnus X-3, 83, 203–206

Darwin instability, 111
delay-time distribution, of Type Ia SNe, 512–513
Delta Cephei, 16
detached binaries, 139–140
donor star: convective envelope, response to mass loss, 95ff, 336; overfilling Roche lobe, 95–98; radiative envelope, response to mass loss, 93ff, 335; response to mass loss, 92ff, 335–336
Doppler effect, 19
double black holes, 3, 9, 25, 26, 652–655; double formation models, 419–433, 489–492, 669–677; final evolution and formation of, 414–425. *See also* black holes; SS433-like mass transfer
double black holes, formation by: CE evolution of wide systems, 414–419, 449–450, 670–672; chemically homogeneous evolution, 673–676; dynamical interactions in star clusters and AGNs, 489–492; stable Roche-lobe overflow evolution, 419–423, 449–450, 673
double-degenerate model of type Ia SNe, 29–30, 505ff, 508, 511–513
double neutron star, 25, 26. *See also* pulsars (radio): binary
double pulsar, 25, 628–630
double white dwarfs, 156–159
dwarf novae, 19, 457
dynamical interactions (in star clusters): direct collision, 483, 486–489; exchange encounter, 487–489; formation of compact-star binaries, 483ff; formation of double BHs, 489–492; globular clusters, 480ff; nuclear star cluster (in AGN), 492; tidal capture, 484–486

eccentricity, 39, 590–591
eclipsing binaries, 15–17, 22, 41–44, 140v142, 151–152
eclipsing binary light curves, 41–44, 140–142, 151–152
Eddington accretion limit, 75, 131–133
Eddington accretion rate, 75, 132, 133
edge-lit detonations, 29, and Chapter 13
Einstein Telescope, 708
electron-capture collapse, 270, 299–301, 518–523. *See also* accretion-induced collapse
electron-capture SNe, 270, 299–301, 518–523
energetics of accretion, 170
envelope, stellar. *See* single stars evolution; stars
equilibrium spin, 238–239
e-Rosita, 7
evolution of stars: binaries, 326ff; single stars, 271ff
eXTP, 7

FAST, 7
fast radio bursts, 224–227
Fraunhofer, J. von, 11
Frost, Robert, 15

GAIA, 11, 509–510
Galilei, Galileo, 10
gamma-ray binaries, 223–224
gamma-ray bursts, 5, 678ff, 712ff, 748–752; long (*see* supernovae, Type Ic-BL); short, 5–6, 712–718. *See also* mergers: neutron stars
globular clusters: black holes, formation, 489–492; compact object binaries, observed, 482–483; core collapse, 489; dynamical interactions between stars, 480ff; formation of compact star binaries, 480ff; kicks to black holes, 492; X-ray sources, 24, 169, 258, 482–483. *See also* pulsars (radio): millisecond
Goodricke, John, 16, 17
gravitational contraction, 271ff. *See also* virial theorem

© Copyright, Princeton University Press. No part of this book may be distributed, posted, or reproduced in any form by digital or mechanical means without prior written permission of the publisher.

gravitational quadrupole moment variations, 83. *See also* Applegate mechanism
gravitational radiation. *See* gravitational waves
gravitational waves: cosmological implications, 717–720; evidence of, from binary pulsars, 625–626, 655–656; kilonova, 714; luminosity, 658–660; merger rates, 664–666, 694–696, 747–752 (*see also* mergers, rates); merger timescale, 660–662; observations, 678ff; signals from binaries, 662–664; sources, continuous, 712, 718–730; sources, detected, 678ff; sources, dual-line, 712ff, 721–725; sources, potential, 659; spectrum, 663, 708–710; strain, 654, 661–664, 732–738
gravitational waves, detectors of LIGO-Virgo-KAGRA network, 652–653, 708; of LISA, 719ff, 820ff
Gunn-Ostriker mechanism, 233

helium stars: detection, 360–366; evolution, 315–325, 366–371, 515–528; formation, 343–353, 360–365; UV-bright LMC stars, 363–365. *See also* binary evolution; R Corona Borealis stars; Wolf-Rayet stars
helium white dwarfs. *See* white dwarfs: helium
Herschell, William, 10, 11
high-mass X-ray binaries (HMXBs), 21–23, 178ff, 213ff; CE-evolution, 123–124, 404–408; Corbet diagram, 243–244; formation, 376ff; formation of systems with black holes, 412–414; galactic distribution, 169, 173; mass determination, 189–192; mass transfer (mechanisms), 182–188; observations and properties, 168ff, 213ff; orbital period distribution, 180; pulse-period distribution, 269; runaway HMXBs (*see* runaway stars); stability of mass transfer, 398; standard HMXBs, 213–223; supergiant fast X-ray transients (SFXTs), 213–223; supergiant high-mass X-ray binaries (sg-HMXBs), 213–223; Wolf-Rayet star donors, WR X-ray binary, 203–207. *See also* black holes
high-mass X-ray binaries, Be/X-ray binaries, 213–217; dichotomous kicks, 82–385; formation, 379–382; formation rate, 376, 402; two populations, 382–385
high-mass X-ray binaries, black-hole systems: final evolution and formation of double black holes, 414–425; formation of, 412–414; observations, 193–197, 246ff
high-mass X-ray binaries, evolution: final outcome of, 123–124, 404–408, 414–428; non-conservative, 403–405, 42–431
high-velocity remnants of Type Ia supernovae, 508–511
Hoyle-Lyttleton accretion, 212
Huggins, W., 11
Hulse, Russell, 3, 625, 655
Hulse-Taylor binary radio pulsar, 655–656
Huygens, C., 33
hypervelocity stars, 509–513, 552–554

incidence of interacting binaries, 51ff
IndIGO, 9, 653
Initial Mass Function, 46
INTEGRAL, 5, 7
interacting binaries, 51ff; incidence, 51–52; mass-ratio distributions, 55–57; orbital period distribution, 53–55; primary mass distribution, 53ff
intermediate-mass X-ray binary, 188, 256, 475–477, 591–594; rarity, reason for, 188; stability of mass transfer, 475–477
iron-core collapse, 302–315
isotropic re-emission, mass transfer, 73ff, 256, 421, 594–595

KAGRA, 9, 652–653
Kepler, J., 33
Kepler's laws, 33, 34
kicks. *See* pulsars (radio): kicks; supernovae, kicks from
kilonova, 5, 6, 653, 713, 714, 715
Kirchhoff, G.R., 11
Kozai-Lidov resonance, 7, 676

© Copyright, Princeton University Press. No part of this book may be distributed, posted, or reproduced in any form by digital or mechanical means without prior written permission of the publisher.

Lagrangian points, Roche equipotentials, 60–70

Laplace, Pierre S., 10

Leavitt, Henriette, 17

LIGO (network), sensitivity curve, 663. *See also* gravitational waves, detectors, sources; LIGO-Virgo-KAGRA-IndIGO

LIGO-India (IndIGO), 9, 653

LIGO-Virgo-KAGRA, 9, 46, 414, 423, 490, 540–541, 640, 641, 643, 653, 667, 668, 680, 695, 701, 706–708, 719

LIGO-Virgo-KAGRA-IndIGO, 9, 652, 653

LIGO-Virgo network, 9

LION, 708

LISA, 9, 326, 718ff; sensitivity, 730–736; sources, 711, 718–730

low-mass X-ray binaries (LMXBs), 24, 25; accreted amount of matter on neutron star, 441; accreting millisecond pulsars, 262–270; with black holes, 195–197; converging, 452, 470–472; diverging, 452, 470–472; Galactic distribution, 169; link to MSPs, 26, 263–268; mass transfer (by RLO), 182ff; mass transfer driven by orbital angular momentum loss, 452–457; mass-transfer mechanisms, 182ff, 450–457, 579–591; observations and properties, 174–178, 258–270; orbital period distribution, 177, 180; orbital period minimum (absence of), 457, 462; quasi-periodic oscillations (*see* quasi-periodic oscillations); stability of mass transfer, 475–477; symbiotic X-ray binaries, 268–270; wide-orbit LMXB mass-transfer mechanisms, 470–476; wide-orbit LMXBs, 470–476; X-ray bursts, 258–261

low-mass X-ray binaries (LMXBs), evolution of: close systems, 450–457; wide systems, 470–476

low-mass X-ray binaries (LMXBs), formation of: by accretion-induced collapse, 436–447, 595–597; by CE evolution, 433–436; LMXBs with BHs, 449–452; LMXBs with NSs, 433–447, 579–591; rate in Galaxy, 433; triple star model, 448–449

luminous blue variables, 293–298

luminous red novae, 128–130

luminous super-soft X-ray sources, 164–167

macronova, 713

magnetar, 5, 385–386, 562

magnetic Ap, Bp stars, origin, 371–374

magnetic braking, 454–457

magnetic field, decay induced by accretion, 439–440, 604–605. *See also* neutron stars; white dwarfs

magnetosphere: interaction with disk, 237–239; radio pulsar, 564, 583, 598, 613; X-ray pulsar, 172, 232–238

Markov chain Monte Carlo method, 746

mass determination: binary components, 41–42; black hole masses, 194–197, 652ff; main-sequence stars, 42–44; neutron stars, using special and general relativity, 616ff

mass function, 42, 173

mass limit (lower, ZAMS) for producing a black hole: binary stars, 411–414; single stars, 411–414

mass limit (upper) for neutron stars, 419

mass loss: modes, 65ff; from red supergiants, 292; by stellar wind, 184–188 (*see also* stellar wind); from Wolf-Rayet stars, 185

mass-luminosity relation, 44

mass-ratio distribution, 55ff, 741–743

mass transfer, 3, 334ff: circumbinary disk, 76ff; conservative, 72ff; driven by internal evolution (*see* low-mass X-ray binaries: mass-transfer mechanism); driven by orbital angular momentum loss (*see* orbital angular momentum balance equation); dynamically unstable, 340; dynamically unstable isotropic re-emission, 73ff, 256, 421, 594–595; Jeans' mode, 71, 78; mechanisms driving mass transfer in LMXBs, 182ff, 450–457, 579–591; response of mass-gaining star, 341–351 (*see also* common envelope); response of mass-losing star, 93ff; stability, criteria for, 91, 92,

© Copyright, Princeton University Press. No part of this book may be distributed, posted, or reproduced in any form by digital or mechanical means without prior written permission of the publisher.

mass transfer (*continued*) 336–339, 475–477; stability in HMXBs, 396–398, 477; stability in IMXBs, 91, 475–477; stable, 339; stellar wind (*see* accretion, stellar wind); in X-ray binaries (*see* high-mass X-ray binaries: mass transfer; low-mass X-ray binaries: mass transfer). See also binary evolution; Roche-lobe overflow
mass transfer, non-conservative, 403–407, 410–411: reasons for, 334ff; response of Roche lobe, 338
Maury, Antonia C., 14
merger rates for compact stars: empirical (double neutron stars), 694–696, 748–752; Galactic (double neutron stars, theoretical), 60, 752–753
mergers: black holes, 3, 664–666; kilonova (*see* kilonova); main-sequence stars, 371–374; multi-messenger, 712–718; neutron stars, 661–666, 715, 717–718; phases of neutron star mergers, 715, 717–718; properties (*see* gravitational waves). *See also* black holes: spin
Michell, J., 10, 11
microquasars, 197ff
millisecond radio pulsars, 26, 27. *See also* pulsars (radio), millisecond
Minkowski, R., 495
Mira Ceti, 163
misalignment angle. *See* pulsars (radio): inclination angle
Mizar, 10, 14–16
Montanari, G., 16
Monte Carlo simulations, 745–746
multi-messenger astrophysics, 712–718
multiplicity factor, 52

neutron stars (NSs): number in Galaxy, 206. *See also* pulsars (radio); pulsars (X-ray); spin, equilibrium; supernovae, kicks from
neutron stars (NSs), double: formation, 305f; mergers, 661–666, 715, 717–718. *See also* pulsars (radio), binary
neutron stars (NSs), magnetic field (dipole), 5, 561, 563, 569–575, 617; decay, by accretion, 439ff
neutron stars (NSs), mass of: maximum, 419; measurements of, 189–192, 630–633; predicted (theory), 304ff
neutron stars (NSs), spin (distribution): binary and millisecond pulsars, 616–617; radio pulsars, general, 5; X-ray pulsars, 269
Newton, Isaac, 11, 33, 35
non-conservative evolution, 8, 356–360, 364–366, 383–385, 403ff, 414ff
non-degenerate binaries, 143–152
novae, 17–19. *See also* black holes; dwarf novae; kilonova; red novae
Nova Her 1934 (DQ Her), 18, 19
nuclear burning phases, 275ff, 301–305

OGLE, 364, 365
orbit (of binary): absolute, 33, 34; relative, 33, 34
orbital angular momentum, 65ff; balance equation, 68ff; loss, 68ff
orbital changes due to mass transfer/loss, 65ff, 77ff
orbital elements, 37ff
orbital period distributions, 53–55
orbit determination, 36ff

pair-instability supernova, 270, 280, 312, 322–325, 517
periastron, 37ff
period gap (cataclysmic variables), 457
period minimum (cataclysmic variables), 458–460
persistent versus transient X-ray binaries, 214–215
Phillips relation, 500, 505–506
physical binary, 10
Pickering, E.C., 14, 16
Pismis 24, 44
planetary nebulae, double nuclei, 154–156
population synthesis. *See* binary population synthesis
pre-supernova structure, 300–305, 514ff
propeller phase, 234–236
pulsars (radio): beaming fraction, 564–565; binary, 3, 25, 26, 560, 571–574, 655, 664–666; binary, companions, 572–573; binary, formation, 404–408, 578–595, 637–647, 664–666;

© Copyright, Princeton University Press. No part of this book may be distributed, posted, or reproduced in any form by digital or mechanical means without prior written permission of the publisher.

binary, masses, 572–573, 631–633; binary masses, black widows, 85, 579–582; characteristic age, 570–571; companions, 571–648; companion types, 577–578, 617; dispersion measure, 567–568; evolutionary tracks, 610–612; galactic distribution, 567; gravity tests (binary pulsars), 618–629, 655–657; inclination angle, 563; kicks, 635 (*see also* supernovae, kicks from); magnetic field (dipole), 5, 561ff, 569–575, 599–601; pulse profiles, 565–566; recycling (spin up), 26, 405, 560, 571–574, 597–604; redbacks, 562, 571, 581–583; spin, 562; spin-down timescale, 570–571, 608–612; spin-period distribution, 615–617; spin-up line, 602–604; stellar evolution (link), 615–618; true ages, 569–570, 608–612

pulsars (radio), millisecond, 5, 26, 560–567; accretion-induced collapse, formation by, 595–596; accretion torques, 598; black widows, 85, 571, 581–582; characteristic age, 608–612; companions, 574–576; decoupling from Roche lobe, 612–614; eccentric, 590–591; formation, 578–589; magnetic fields, 599–601; masses, 631–633; orbital periods (long), 585–589; orbital periods (short), 579–585, 591–596; populations, 574–576; redbacks, 562, 571, 581–583; Roche-lobe decoupling, 612–614; spin-period distribution, 615–617; spin-up line(s), 601–604; submillisecond, 614; true age, *608–612*; ultra-light companion, *578–583*

pulsars (X-ray), 21–23, 178; accreting millisecond pulsars, 24, 26, 263–266, 560; orbit determination, 21–22, 188–191; pulse period distribution, 269; pulse profiles, 178

pulsational pair-instability supernovae, 322–324, 667–669

quadrupole moment (gravitational), 80

quasi-periodic oscillations (QPOs), 261ff: kHz QPOs, 262–266

Quintiplet cluster, 45

radial velocity, 38ff: curves of, 21–22, 40, 41, 48, 50, 619, 655; falsification of curves of, 46ff

radio pulsars. *See* pulsars (radio)

R Corona Borealis (R Cor Bor) stars, 361–362

recycled pulsars, 26

recycling. *See* pulsars (radio): recycling

redbacks. *See* pulsars (radio), millisecond: redbacks

red novae, 128–130. *See also* common envelope; luminous red novae

redshift, 14

red supergiants, 296–298. *See also* Conti scenario

relative orbit, 12, 34

relativistic objects (in binaries), 22. *See also* black holes; pulsars (radio)

RGB, 328

Roche equipotentials, 59ff, 63, 69; Lagrangian points of, 60–70

Roche lobe, 7, 61f; decoupling from, 612–614; definition, 61; response to mass transfer and mass loss, 92ff

Roche-lobe overflow (RLO), 63ff: atmospheric, 90ff; Cases A, B, C, AB, BB (*see* binary evolution, individual cases); non-conservative, 359–360; stability criteria, 91–92 (*see also* binary evolution, stability of mass transfer of); unstable (*see* binary evolution; mass transfer: stability); in X-ray binaries, 182ff

Rossiter-McLaughlin effect, 49

Rotation: effect on stellar evolution, 287–290; rotation effect, 49

r-process elements, 5, 653, 717–718

RRAT, 5, 562

RS CVn stars, 86

runaway stars, 380–395, 541–554; OB-runaways, 389–393; X-ray binaries, 393–395; zombie stars (SN Ia remnants), 509

Sco X-1, 21, 176

semi-detached binaries, 139, 141, 144

semi-major axis, 34ff

semi-minor axis, 34ff

settling accretion, 231–233

short Gamma-Ray Burst, 5–6, 712–718

© Copyright, Princeton University Press. No part of this book may be distributed, posted, or reproduced in any form by digital or mechanical means without prior written permission of the publisher.

single-degenerate model. *See* supernovae, Type Ia single degenerate model
single stars, evolution of: evolutionary tracks, 281, 285–291; evolution of core, 279; evolution of radius as function of metallicity, 293; evolution of radius of 5 solar mass star, 283; final outcome (white dwarfs, neutron star or black hole), globally, 298–305; final outcome for stars, 8 solar masses, detailed computations, 305–315; hydrogen burning, beyond, 276–284; overview, 271–290; rotation, effects of, 287–290; wind mass loss, effects of, 284–289
Sirius AB, 11–13, 31
slowly-rotating early-type main sequence stars, origin, 371–374
spectroscopic binaries, 14, 140; orbital elements, 37; orbit determination, 38–41; radial velocity curves, 40, 41, 48
spin: black-hole GW mergers (measured), 696–707; black holes in X-ray binaries, 245–252; equilibrium (neutron star), 238–239; period distribution X-ray binaries, 269; period distribution millisecond radio pulsar binaries, 615
spin-evolution: accreting neutron star, 239–243, 601–617; black holes, expected from single stellar evolution, 704–707; black holes in X-ray binary, 696–707
spin-orbit couplings, 80ff, 85ff
Square Kilometer Array (SKA), 7
SS433, 199–206, 419–425
SS433-like mass transfer, 419–425; formation of double black holes, 419–425
stable mass transfer Roche-lobe overflow HMXBs, 419–425
stars: Ap/Bp and slow rotators, origin of, 371–374; binaries, evolution of (*see* binary evolution); mergers of non-compact stars, 371–374 (*see also* red novae); nuclear burning (phases), 274–277; rotation effects, 287–290; single stars versus binaries, final outcome of, 366–371; stellar timescales, three, 274–276; wind mass loss (effects), 284–289. *See also* donor star; helium stars; single stars; spin evolution: accreting neutron star
stars, mass determination of: black holes (*see* black holes: masses); main sequence stars, 42–44; metallicity effects, 285–288, 293; neutron stars (*see* neutron stars, mass of)
stellar evolution: binaries, 326ff; single stars, 271ff
stellar wind: accretion of, 72, 184–188, 227–231; from massive stars, 184–188; mass-loss rates, 185; red supergiants, 292; velocities, 185, 186; Wolf-Rayet stars, 185
supergiant fast X-ray transients (SFXTs), 213–223. *See also* high-mass X-ray binaries
supernova (SN). *See* supernovae
supernovae (SNe), 6, 27–29, 485ff; asymmetric, 531–538; disruption of binary, 78–80, 534–555; electron capture, 270, 299–301, 518–523; explosion mechanism, 301–315, 531; failed supernovae, 315; iron-core collapse, 299–315; kinematic impact, 541–555; kinematic impact of orbital changes, 544–547; light curves, 497, 500, 505, 526; neutron star or black hole, as remnants, 301–315, 369–378; observational properties, 495–501; orbital changes (due to supernovae in binaries), 78–80, 544–547; pair instability, 270, 280, 312, 322–325, 517; pre-supernova structure, 300–305, 514ff; pulsational-pair instability, 322–324, 667–669; rates, 496, 498, 512; remnants, 392, 509–511; runaway stars (*see* runaway stars); shell impact, 522–555; spectra, 495–496; stripped envelope, 496, 513–518; supernova 1987A, 27, 497; symmetric ejection, effects on orbit, 78–80; thermonuclear, 30, 291, 498–513; ultra-stripped, 523–529
supernovae, core collapse, 27–29, 301–315: examples of model outcomes, 30–315, 369–370
supernovae, kicks from, 531–556; effects on binary orbits, 541–556; from electron capture, 537–538;

© Copyright, Princeton University Press. No part of this book may be distributed, posted, or reproduced in any form by digital or mechanical means without prior written permission of the publisher.

observational evidence, 532–534; theoretical reasons, 534–536; from ultra-stripped supernovae, 538–539
supernovae, kicks of black holes, 492–494, 539–541
supernovae, kicks of neutron stars, 382–385, 534–555; dichotomous kicks, 382–385, 537–538; from electron-capture collapse, 537–538; kick-mass correlation (NSs), 538–539; from ultra-stripped cores, 538–539
supernovae, Type Ia, 6, 28–30, 498–513; Chandrasekhar-mass models, 29, 502ff; deflagration-detonation model, 502; delayed detonation model, 502; delay-time distribution, 512–513; double-degenerate model, 29–30, 505ff, 508, 511–513; edge-lit detonations, 503–506; high-velocity remnants, 508–511; light curves, 497, 500; only deflagration model, 502; Phillips relation, 500, 504, 506; single degenerate model, 29–30, 507–508, 511–513; spectra, 495, 496, 499; sub-Chandrasekhar mass models, 503–506; zombie star (partly consumed WD remnant), 509
supernovae, Type Iax, 501, 510
supernovae, Type Ib/c, 27–28, 495–498
supernovae, Type Ic-BL, 495, 497
supernovae, Type II, 27–28, 495–498
super-soft X-ray sources, 164–167
Swift, 7
symbiotic stars, 3, 141, 161–163
symbiotic X-ray binaries, 268–270; mechanisms driving the mass transfer, 470–476
symmetric mass ejection (effect on orbit). *See* supernovae: symmetric ejection
systemic velocity (after symmetric supernova), 80

Tayi, 653
Taylor, J.H., 3, 625, 655
thermal pulses, 163
thermonuclear supernova explosions. *See* supernovae, Type Ia
thermonuclear X-ray bursts, 258–261
Thorne, K., 3, 625
Thorne-Zytkow objects, 123, 407–409
Tian Qin, 9, 653
tidal capture, 48–486
tidal dissipation (convective zone), 113–114
tidal dissipation (radiative zone), 114–115
tidal evolution (of binaries), 109ff
tides: dynamical, 114; equilibrium, 110ff; timescale circularization, 115; timescale synchronization, 115, 705–707
transient sources: Be/X-ray transients, 214–217; black hole X-ray transients, 193–196 (*see also* X-ray novae); optical transients, 713–718; supergiant X-ray transients, (SFXTs), 221–223
triple pulsar, 6, 587–589
triple-star model for formation of LMXBs. See low-mass X-ray binaries, formation of
triple systems, 6, 52, 207

UHURU satellite, 21
ultra-compact X-ray binaries (UCXBs), 267–268: evolution, 462–470; formation, 462–470; observations, 267–268
ultra-luminous X-ray binaries, 252–258
ultra-stripped supernovae, 523–529
unevolved binaries, 143–144
UV-bright LMC stars, 363–365; as progenitors of LMXBs, IMXBs, 365–366

van de Kamp, P., 13
Virgo: *See*: LIGO-Virgo-KAGRA, LIGO-Virgo-KAGRA-IndIGO and LIGO-Virgo network
virial theorem, 80, 104, 271–274; and: gravitational contraction phases, 271–274; and nuclear burning phases, 274–275; and over-all stellar evolution, 274–275
visual binaries, 10, 11, 114

Walker, M. F., 18, 19
Webbink diagram, 331–333
Weiss, R., 3, 625
Westerlund, 1, 44
white dwarfs: accretion limit (Eddington), 153; carbon-oxygen (CO), 572ff, 590ff; double, 156–159; helium, 159ff, 343–346, 585–590; magnetic,

© Copyright, Princeton University Press. No part of this book may be distributed, posted, or reproduced in any form by digital or mechanical means without prior written permission of the publisher.

white dwarfs (*continued*)
  160; orbital period, mass correlation of helium with, 472–476, 585–590; oxygen-neon-magnesium (O-Ne-Mg), 572ff, 590ff (*see also* accretion-induced collapse; supernovae, electron-capture); radio pulsating, 161
WN3/O3 stars, 363–365
Wolf-Rayet (WR) stars, 45ff, 146–149; formation of, 377–379, 386–389; mass-loss rates of, 185; spectra, 45; WR binaries, 146–149, 386–389; WR Galaxy, 151; WR X-ray binary, 203–207. *See also* helium stars
WR-star. *See* Wolf-Rayet stars

XDIN, 5, 562
XMM-Newton, 7
X-ray binaries: discovery of, 21–25; Galactic distribution, 21, 169, 173; observed properties, 168, 174–178, 258–270, 213ff; orbital period distribution, 180; orbital sizes, 179. *See also* black holes; high-mass X-ray binaries; low-mass X-ray binaries; symbiotic X-ray binaries; Wolf-Rayet stars, WR X-ray binary
X-ray bursts, 258–261: burst oscillations of, 265–266; thermonuclear (Type I), 258–261
X-ray novae. *See* black holes; high-mass X-ray binaries; novae
X-ray pulsars. *See* pulsars (X-rays)

Yellow supergiants/hypergiants, 295

Zero-Age Main Sequence (ZAMS), 54ff, 279, 291
ζ and ε Aurigae stars, 150–152
Zeta Aurigae binaries, 150–152
zombie star, 509. *See also* supernovae, Type Ia
Zwicky, F., 27, 495